Quantitative Ambiguity Analysis for Matched-Field Source Localization under Spatially-Correlated Noise Field

Wen Xu[†] and Christ D. Richmond[‡]

[†] RD Instruments
9855 Businesspark Ave
San Diego, CA 92131, USA
wxu@rdinstruments.com

[‡] Lincoln Laboratory
Massachusetts Institute of Technology
244 Wood Street, Rm S4-317
Lexington, MA 02420, USA
christ@ll.mit.edu

Abstract-Matched-field methods find source location by matching the measured signal field with the modeled signal field. The resulted ambiguity output is often characterized by a multimodal structure. At high signal-to-noise ratio (SNR), the peak at the true source position is a global maximum and can be located accurately; below some threshold SNR, the true peak is easily obscured by other ambiguous peaks, leading to a significantly increased localization error. To analyze this threshold performance behavior, a quantitative approach for error analysis has previously been developed in the context of the maximum likelihood estimate (MLE) with spatially-white noise [1, 4]. In this paper, the same approach is generalized to work for spatially-correlated noise field introduced by discrete interferences and/or surface distribution sources.

I. Introduction

Matched-field processing (MFP) concerns estimation of source location by exploiting full wave modeling of acoustic waveguide propagation [2]. The ambiguity output in MFP relies on the correlation between the signal field at the true source position and the signal field at each scanning source position. This correlation often shows a multimodal structure due to the nonlinear parameter dependence: in addition to a mainlobe around the true source position, there are unpredictable prominent high sidelobes elsewhere. For a well-conditioned problem, in the absence of noise the peak output is guaranteed to occur at the true source position. In the presence of noise, we will probably have some peak outputs around the sidelobes, introducing a large localization error. Therefore, output ambiguity structure is a very important factor in the development of any matched-field algorithm operated in low SNR scenarios.

A few parameter estimation performance bounds have been developed to predict the threshold SNR below which the sidelobe errors dominate the matched-field performance [3, 4]. Evaluation of those bounds, however, is often subject to numerical sensitivity otherwise quite demanding in computation.

A quantitative approach for matched-field ambiguity analysis has been introduced in the context of the maximum likelihood estimate, which explicitly exploits the signal ambiguity structure and applies error analysis in the likelihood ratio test (LRT) [1, 4]. It only requires some coarse information on the signal field correlation and has a simple physical interpretation and implementation. Some similar approaches have also been investigated in the bearing estimation problem [5, 6]. Despite the simple implementation, the error analysis based on the LRT has shown very promising results, predicting mean-square error performance of MLE with remarkable accuracy well into the threshold region. Most current research, however, mainly considers spatially-white noise process. The colored noise case is only recently studied in bearing estimation with deterministic signal component [7].

The ambient noise in the ocean is often spatially correlated originating from discrete interferences (shipping and other man-made sources) or surface-generated distribution sources. In this paper, we generalize the approach in Ref. [1] to include such colored noise field.

II. Matched-Field Problem

Consider a stratified waveguide model consisting of water column, multi-layer sediment and semi-infinite basement, either range-dependent or independent (see Fig. 1). A point source radiates narrow-band or broad-band signals, and the signal field is sampled by a vertical receiving array. For a stationary random source process, individual frequency bins are uncorrelated with each other. Suppose we have L independent measurements for

0-933957-31-9

each of M frequencies, f_m, m=1, 2, ..., M. A typical receiving data model is expressed as [8]:

$$\mathbf{r}_l(f_m,\boldsymbol{\theta}_s,\boldsymbol{\theta}_{env}) = \tilde{b}_l(f_m)\mathbf{g}(f_m,\boldsymbol{\theta}_s,\boldsymbol{\theta}_{env}) + \mathbf{n}_l(f_m,\boldsymbol{\theta}_{env}), \quad l=1,\ldots,L,\ m=1,\ldots,M, \tag{1}$$

where

$\boldsymbol{\theta}_s$ denotes the unknown source location;

$\boldsymbol{\theta}_{env}$ denotes the environmental parameter set;

$\mathbf{r}_l(f_m,\boldsymbol{\theta}_s,\boldsymbol{\theta}_{env})$ is an N×1 vector representing the l-th snapshot and N is the number of receiving sensors;

$\tilde{b}_l(f_m)$ is a random process incorporating amplitude and phase variability of the source;

$\mathbf{g}(f_m,\boldsymbol{\theta}_s,\boldsymbol{\theta}_{env})$ is a vector of Green's function for the propagation from the source to the receiving array; and

$\mathbf{n}_l(f_m,\boldsymbol{\theta}_{env})$ is the l-th snapshot of the observation noise.

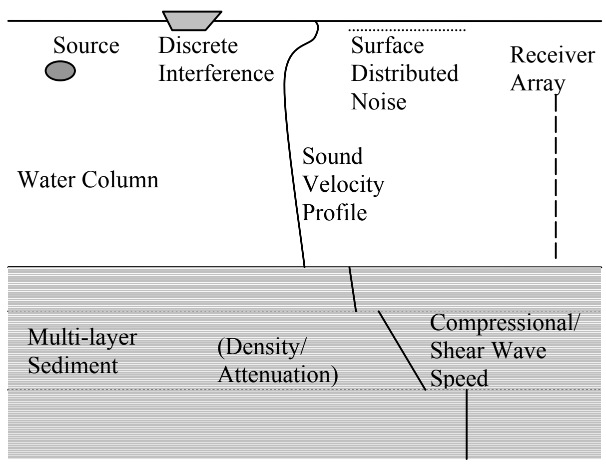

Figure 1 Typical environmental model for matched-field processing. Receiving system configuration is also shown.

In Ref. [1], only the measurement noise is discussed, which is spatially white. As mentioned in Section I, in most practical situations some other interferences co-exist in the propagation environment, either spatially discrete like artificial interfering sources or continuous like the surface-generated sources by wind. In those cases, the noise can often be represented by two terms, one spatially white and one spatially correlated:

$$\mathbf{n}_l(f_m,\boldsymbol{\theta}_{env}) = \mathbf{n}_{cl}(f_m,\boldsymbol{\theta}_{env}) + \mathbf{n}_{wl}(f_m). \tag{2}$$

Both the signal and noise terms are assumed to follow a zero-mean complex Gaussian distribution. The stationary noise process is as well uncorrelated across the signal frequency band and independent of the signal process. Under those assumptions, the covariance matrix of $\mathbf{r}_l(f_m)$ [1] has the form of

$$\mathbf{K}_\mathbf{r}(f_m,\boldsymbol{\theta}_s) = \sigma_b^2(f_m)\mathbf{g}(f_m,\boldsymbol{\theta}_s)\mathbf{g}^H(f_m,\boldsymbol{\theta}_s) + \mathbf{K}_\mathbf{n}(f_m), \tag{3}$$

where $()^H$ denotes the complex conjugate transpose operation and $\sigma_b^2(f_m)$ is the variance of the signal process. The noise contribution can be further written as

$$\mathbf{K}_n(f_m) = \mathbf{K}_{cn}(f_m) + \sigma_{wn}^2(f_m)\mathbf{I}, \tag{4}$$

where $\sigma_{wn}^2(f_m)$ denotes the variance of the white noise process.

Denote the entire observation by

$$\mathbf{r} = \left[\mathbf{r}_1^T(f_1) \quad \ldots \quad \mathbf{r}_L^T(f_1) \quad \ldots \quad \mathbf{r}_1^T(f_M) \quad \ldots \quad \mathbf{r}_L^T(f_M)\right]^T. \tag{5}$$

Given known source location, the probability density function of $\mathbf{r}$ is

$$p(\mathbf{r}\,|\,\boldsymbol{\theta}_s) = \frac{1}{\prod_{m=1}^M \left|\pi\mathbf{K}_\mathbf{r}(f_m,\boldsymbol{\theta}_s)\right|^L}\prod_{m=1}^M\prod_{l=1}^L \exp\left(-\operatorname{tr}\left(\mathbf{K}_\mathbf{r}^{-1}(f_m,\boldsymbol{\theta}_s)\mathbf{r}_l(f_m)\mathbf{r}_l^H(f_m)\right)\right). \tag{6}$$

The maximum likelihood estimate of $\boldsymbol{\theta}_s$ is obtained by maximizing the logarithm of the conditional probability density function in (6) with respect to $\boldsymbol{\theta}_s$. For white noise process, the MLE is previously derived as [1]:

$$\hat{\boldsymbol{\theta}}_{s-ML}(\mathbf{r}) = \arg\max_{\boldsymbol{\theta}_s} \sum_{m=1}^M\sum_{l=1}^L \left|\mathbf{r}_l^H(f_m)\mathbf{g}_\mathrm{n}(f_m,\boldsymbol{\theta}_s)\right|^2, \tag{7}$$

where $\mathbf{g}_\mathrm{n}(f_m,\boldsymbol{\theta}_s)$ is the normalized Green's function, i.e.,

$$\mathbf{g}_\mathrm{n}(f_m,\boldsymbol{\theta}_s) = \frac{\mathbf{g}(f_m,\boldsymbol{\theta}_s)}{\left\|\mathbf{g}(f_m,\boldsymbol{\theta}_s)\right\|} \tag{8}$$

and $\|\cdot\|$ is the norm of a complex vector. Note that Eq. (7) is another form of the conventional matched-field processor [2]. The MLE output in (7) is a function of the signal field correlation defined by

$$\Gamma(f,\boldsymbol{\theta}_s,\boldsymbol{\theta}_{s0}) = \left|\mathbf{g}_\mathrm{n}^H(f,\boldsymbol{\theta}_s)\mathbf{g}_\mathrm{n}(f,\boldsymbol{\theta}_{s0})\right|^2, \tag{9}$$

[1] For notational convenience, $\boldsymbol{\theta}_s$ and/or $\boldsymbol{\theta}_{env}$ are sometimes removed from variable expressions.

where $\boldsymbol{\theta}_s$ and $\boldsymbol{\theta}_{s0}$ denote the true and scanning parameter sets, respectively. The function in (9) is often called the signal ambiguity function (beampattern in DOA estimation) due to its multimodal structure as a function of $\boldsymbol{\theta}_s$, which comes from the nonlinear dependence of the signal field on the embedded parameters.

III. Review of Maximum Likelihood Error Analysis

To directly connect the multimodal ambiguity structure with the error in source localization, a probabilistic approach is developed for error analysis of the maximum likelihood estimate [1]. Consider a discrete set of scanning parameter points, $\{\boldsymbol{\theta}_{s1}, \boldsymbol{\theta}_{s2}, \ldots\}$, and suppose the true parameter point is one of them, $\boldsymbol{\theta}_{sj}$. It is shown that the exact error probability at any scanning point $\boldsymbol{\theta}_{sk} \neq \boldsymbol{\theta}_{sj}$ is, by the first-order approximation, the error probability of the likelihood ratio test (LRT) associated with $\boldsymbol{\theta}_{sk}$ and $\boldsymbol{\theta}_{sj}$. For the white noise model, given the true parameter at $\boldsymbol{\theta}_{sj}$, the LRT error probability is readily available from (7), which is

$$\mathrm{P_e}(\boldsymbol{\theta}_{sk}|\boldsymbol{\theta}_{sj}) = \Pr\left(\sum_{m=1}^{M}\sum_{l=1}^{L}\left|\mathbf{r}_l^H(f_m)\mathbf{g}_\mathrm{n}(f_m,\boldsymbol{\theta}_{sk})\right|^2 > \sum_{m=1}^{M}\sum_{l=1}^{L}\left|\mathbf{r}_l^H(f_m)\mathbf{g}_\mathrm{n}(f_m,\boldsymbol{\theta}_{sj})\right|^2\right). \tag{10}$$

The approximation is particularly good at moderate to high SNR. Multiplying it by the corresponding distance square yields the estimation error at each scanning point, which we call the probabilistic square error.

For the single-parameter case, given the true parameter at θ_{sj}, the estimation error at θ_{sk} ($k \neq j$) is

$$\varepsilon^2_{\mathrm{MLE}}(\theta_{sk}|\theta_{sj}) \approx \mathrm{P_e}(\theta_{sk}|\theta_{sj}) \times (\theta_{sk} - \theta_{sj})^2. \tag{11}$$

Errors at different mainlobe/sidelobe points can then be compared by choosing θ_{sk} accordingly. To locate the threshold SNR, at each SNR a representative ambiguity point is identified by locating the peak of the probabilistic square error; the threshold SNR is defined as the SNR at which the representative ambiguity point switches from a mainlobe point to a sidelobe point.

In multiple parameter estimation, the ambiguity points are dispersed on a multi-dimensional ambiguity surface. To study the effect of the mainlobe and sidelobes (distributed in a multi-dimensional space) to the estimation of one particular parameter, the ambiguity function for multiple parameters needs to be projected onto the dimension of the designated parameter. For each realization of that parameter, the projected ambiguity level is the multi-dimensional one maximized over other parameter intervals. Error analysis can then be implemented based on this projected one-dimensional ambiguity function following exactly the same way as for the single-parameter one-dimensional problem. This provides an attractive framework to investigate the effect of environmental uncertainty to source localization.

The above error analysis also leads to a good approximation to the mean-square error of the MLE [4, 5, 6, 7]. Note that in the high SNR region, the peak of the true parameter protrudes prominently above the noise and can be located accurately. The estimation error is due to slight, noise-introduced distortion of the true peak and can be well predicted by the Cramer-Rao bound [8]. In the low SNR region, the true peak could be below the noise level and obscured by other ambiguous peaks. A larger error arises when a wrong peak is selected.

For the single-parameter case we can divide the parameter interval into multiple (N_{int}) sub-intervals so that, except the mainlobe sub-interval, each sub-interval contains an apparent sidelobe structure. Previously different sidelobe errors corresponding to different sub-intervals are uniformly treated [9, pages 273-286]. To achieve a better approximation, we denote each sub-interval by the sidelobe peak point, θ_{si}, $i = 1,\ldots,N_{\mathrm{int}}-1$, and use the LRT error probability, $\mathrm{P_e}(\theta_{si}|\theta_{s0})$, as the probability that an estimate falls into this subinterval. Then the mean-square error for the given true parameter θ_{s0} can be approximated by

$$\begin{aligned}\varepsilon^2_{\mathrm{MLE}}(\theta_{s0}) \approx &\left(1 - \sum_{i=1}^{N_{\mathrm{int}}-1}\mathrm{P_e}(\theta_{si}|\theta_{s0})\right) \times \mathrm{CRB}(\theta_{s0}) \\ &+ \sum_{i=1}^{N_{\mathrm{int}}-1}\left(\mathrm{P_e}(\theta_{si}|\theta_{s0}) \times (\theta_{si} - \theta_{s0})^2\right)\end{aligned}. \tag{12}$$

The problem is now simplified to finding the LRT error probability. To make (11) and (12) accurate, an exact closed-form expression for the LRT error probability is desired, which also facilitate the implementation of error analysis. Previously, such an analytic form is solved for white noise process [1, 4]. The results show that the probabilistic error at each scanning parameter point is determined by the signal field correlation level, the SNR, as well as the distance to the true parameter point. In the next section, we derive this error probability for the general noise model in (2) so that the above error analysis approach can be applied to spatially-correlated noise field.

IV. LRT Error Probability under Spatially-Correlated Noise Field

To simplify the math presentation, we consider a single frequency component at f_0. Derivation for multiple-frequency component is quite similar. We derive $\mathrm{P_e}(\boldsymbol{\theta}_{s1}|\boldsymbol{\theta}_{s0})$ in the sequel; to evaluate (11) or (12), one can replace $\boldsymbol{\theta}_{s0}$ and $\boldsymbol{\theta}_{s1}$ accordingly.

Denote

$$\mathbf{R}(f_0)=\left[\mathbf{r}_1(f_0)\quad \ldots \quad \mathbf{r}_L(f_0)\right]. \tag{13}$$

The log conditional pdf can be written as

$$\begin{aligned}&\ln p(\mathbf{r}\,|\,\boldsymbol{\theta}_s)=\\&-L\ln(|\,\pi\mathbf{K}_\mathbf{r}(f_0)\,|)-\mathrm{tr}\left(\mathbf{K}_\mathbf{r}^{-1}(f_0)\mathbf{R}(f_0)\mathbf{R}^H(f_0)\right)\end{aligned}. \tag{14}$$

The log likelihood ratio is simply

$$l(\mathbf{r})=\ln p(\mathbf{r}\,|\,\boldsymbol{\theta}_{s1})-\ln p(\mathbf{r}\,|\,\boldsymbol{\theta}_{s0}), \tag{15}$$

and the covariance matrix under $\boldsymbol{\theta}_{s0}$ and $\boldsymbol{\theta}_{s1}$ are given by

$$\mathbf{K}_\mathbf{r}(f_0|\boldsymbol{\theta}_{s0})=\sigma_b^2(f_0)\mathbf{g}(f_0,\boldsymbol{\theta}_{s0})\mathbf{g}^H(f_0,\boldsymbol{\theta}_{s0})+\mathbf{K}_\mathbf{n}(f_0), \tag{16}$$

$$\mathbf{K}_\mathbf{r}(f_0|\boldsymbol{\theta}_{s1})=\sigma_b^2(f_0)\mathbf{g}(f_0,\boldsymbol{\theta}_{s1})\mathbf{g}^H(f_0,\boldsymbol{\theta}_{s1})+\mathbf{K}_\mathbf{n}(f_0), \tag{17}$$

respectively.

Note that the inverse is given by

$$\mathbf{K}_\mathbf{r}^{-1}(f_0)=\mathbf{K}_\mathbf{n}^{-1}(f_0)-\frac{\mathbf{K}_\mathbf{n}^{-1}(f_0)\mathbf{g}(f_0)\mathbf{g}^H(f_0)\mathbf{K}_\mathbf{n}^{-1}(f_0)}{1/\sigma_b^2(f_0)+\mathbf{g}^H(f_0)\mathbf{K}_\mathbf{n}^{-1}(f_0)\mathbf{g}(f_0)}. \tag{18}$$

Thus the trace can be written as

$$\begin{aligned}\mathrm{tr}\left(\mathbf{K}_\mathbf{r}^{-1}(f_0)\mathbf{R}(f_0)\mathbf{R}^H(f_0)\right)&=\mathrm{tr}\left(\mathbf{K}_\mathbf{n}^{-1}(f_0)\mathbf{R}(f_0)\mathbf{R}^H(f_0)\right)\\&-\frac{\mathbf{g}^H(f_0)\mathbf{K}_\mathbf{n}^{-1}(f_0)\mathbf{R}(f_0)\mathbf{R}^H(f_0)\mathbf{K}_\mathbf{n}^{-1}(f_0)\mathbf{g}(f_0)}{1/\sigma_b^2(f_0)+\mathbf{g}^H(f_0)\mathbf{K}_\mathbf{n}^{-1}(f_0)\mathbf{g}(f_0)}\end{aligned}. \tag{19}$$

Similarly we have for the determinant

$$\begin{aligned}&|\,\mathbf{K}_\mathbf{r}(f_0)\,|\\&=\left|\mathbf{K}_\mathbf{n}^{1/2}(f_0)\left(\mathbf{I}+\sigma_b^2(f_0)\mathbf{K}_\mathbf{n}^{-1/2}(f_0)\mathbf{g}(f_0)\mathbf{g}^H(f_0)\mathbf{K}_\mathbf{n}^{-1/2}(f_0)\right)\mathbf{K}_\mathbf{n}^{1/2}(f_0)\right|\\&=\left|\mathbf{K}_\mathbf{n}(f_0)\right|\left|\mathbf{I}+\sigma_b^2(f_0)\mathbf{K}_\mathbf{n}^{-1/2}(f_0)\mathbf{g}(f_0)\mathbf{g}^H(f_0)\mathbf{K}_\mathbf{n}^{-1/2}(f_0)\right|\\&=\left|\mathbf{K}_\mathbf{n}(f_0)\right|\left(1+\sigma_b^2(f_0)\mathbf{g}^H(f_0)\mathbf{K}_\mathbf{n}^{-1}(f_0)\mathbf{g}(f_0)\right).\end{aligned} \tag{20}$$

Denote

$$\alpha(f_0,\boldsymbol{\theta}_s)=1/\sigma_b^2(f_0)+\mathbf{g}^H(f_0,\boldsymbol{\theta}_s)\mathbf{K}_\mathbf{n}^{-1}(f_0)\mathbf{g}(f_0,\boldsymbol{\theta}_s). \tag{21}$$

The likelihood ratio is then

$$l(\mathbf{r})=L\ln\frac{\alpha(f_0,\boldsymbol{\theta}_{s0})}{\alpha(f_0,\boldsymbol{\theta}_{s1})}+\gamma(f_0,\boldsymbol{\theta}_{s0},\boldsymbol{\theta}_{s1}), \tag{22}$$

where

$$\begin{aligned}&\gamma(f_0,\boldsymbol{\theta}_{s0},\boldsymbol{\theta}_{s1})=\\&\frac{1}{\alpha(f_0,\boldsymbol{\theta}_{s1})}\mathbf{g}^H(f_0,\boldsymbol{\theta}_{s1})\mathbf{K}_\mathbf{n}^{-1}(f_0)\mathbf{R}(f_0)\mathbf{R}^H(f_0)\mathbf{K}_\mathbf{n}^{-1}(f_0)\mathbf{g}(f_0,\boldsymbol{\theta}_{s1})\\&-\\&\frac{1}{\alpha(f_0,\boldsymbol{\theta}_{s0})}\mathbf{g}^H(f_0,\boldsymbol{\theta}_{s0})\mathbf{K}_\mathbf{n}^{-1}(f_0)\mathbf{R}(f_0)\mathbf{R}^H(f_0)\mathbf{K}_\mathbf{n}^{-1}(f_0)\mathbf{g}(f_0,\boldsymbol{\theta}_{s0})\\&=\mathbf{tr}\Big(\mathbf{R}(f_0)\mathbf{R}^H(f_0)\\&\Big[\frac{1}{\alpha(f_0,\boldsymbol{\theta}_{s1})}\mathbf{K}_\mathbf{n}^{-1}(f_0)\mathbf{g}(f_0,\boldsymbol{\theta}_{s1})\mathbf{g}^H(f_0,\boldsymbol{\theta}_{s1})\mathbf{K}_\mathbf{n}^{-1}(f_0)\\&-\frac{1}{\alpha(f_0,\boldsymbol{\theta}_{s0})}\mathbf{K}_\mathbf{n}^{-1}(f_0)\mathbf{g}(f_0,\boldsymbol{\theta}_{s0})\mathbf{g}^H(f_0,\boldsymbol{\theta}_{s0})\mathbf{K}_\mathbf{n}^{-1}(f_0)\Big]\Big).\end{aligned} \tag{23}$$

Recall that we are assuming $\boldsymbol{\theta}_{s0}$ is true. Thus

$$\mathbf{R}(f_0)=\mathbf{K}_\mathbf{r}^{1/2}(f_0,\boldsymbol{\theta}_{s0})\mathbf{Z}(f_0) \tag{24}$$

is actually a whitening operation so that each new snapshot, $\mathbf{z}_l(f_0)$, is complex Gaussian with identity covariance matrix. We then have

$$\begin{aligned}&\gamma(f_0,\boldsymbol{\theta}_{s0},\boldsymbol{\theta}_{s1})=\mathrm{tr}\Big(\mathbf{Z}(f_0)\mathbf{Z}^H(f_0)\\&\mathbf{K}_\mathbf{r}^{1/2}(f_0,\boldsymbol{\theta}_{s0})\Big[\frac{1}{\alpha(f_0,\boldsymbol{\theta}_{s1})}\mathbf{K}_\mathbf{n}^{-1}(f_0)\mathbf{g}(f_0,\boldsymbol{\theta}_{s1})\mathbf{g}^H(f_0,\boldsymbol{\theta}_{s1})\mathbf{K}_\mathbf{n}^{-1}(f_0)\\&-\frac{1}{\alpha(f_0,\boldsymbol{\theta}_{s0})}\mathbf{K}_\mathbf{n}^{-1}(f_0)\mathbf{g}(f_0,\boldsymbol{\theta}_{s0})\mathbf{g}^H(f_0,\boldsymbol{\theta}_{s0})\mathbf{K}_\mathbf{n}^{-1}(f_0)\Big]\mathbf{K}_\mathbf{r}^{1/2}(f_0,\boldsymbol{\theta}_{s0})\Big)\end{aligned} \tag{25}$$

Denote by matrix eigen-decomposition

$$\begin{aligned}&\mathbf{K}_\mathbf{r}^{1/2}(f_0,\boldsymbol{\theta}_{s0})\Big[\frac{1}{\alpha(f_0,\boldsymbol{\theta}_{s1})}\mathbf{K}_\mathbf{n}^{-1}(f_0)\mathbf{g}(f_0,\boldsymbol{\theta}_{s1})\mathbf{g}^H(f_0,\boldsymbol{\theta}_{s1})\mathbf{K}_\mathbf{n}^{-1}(f_0)\\&-\frac{1}{\alpha(f_0,\boldsymbol{\theta}_{s0})}\mathbf{K}_\mathbf{n}^{-1}(f_0)\mathbf{g}(f_0,\boldsymbol{\theta}_{s0})\mathbf{g}^H(f_0,\boldsymbol{\theta}_{s0})\mathbf{K}_\mathbf{n}^{-1}(f_0)\Big]\mathbf{K}_\mathbf{r}^{1/2}(f_0,\boldsymbol{\theta}_{s0}),\\&=\mathbf{U}^H\boldsymbol{\Lambda}\mathbf{U}\end{aligned} \tag{26}$$

which shares the same eigen-values with

$$\begin{aligned}&\Big[\frac{1}{\alpha(f_0,\boldsymbol{\theta}_{s1})}\mathbf{g}(f_0,\boldsymbol{\theta}_{s1})\mathbf{g}^H(f_0,\boldsymbol{\theta}_{s1})-\frac{1}{\alpha(f_0,\boldsymbol{\theta}_{s0})}\mathbf{g}(f_0,\boldsymbol{\theta}_{s0})\mathbf{g}^H(f_0,\boldsymbol{\theta}_{s0})\Big]\\&\mathbf{K}_\mathbf{n}^{-1}(f_0)\mathbf{K}_\mathbf{r}(f_0,\boldsymbol{\theta}_{s0})\mathbf{K}_\mathbf{n}^{-1}(f_0).\end{aligned} \tag{27}$$

This is obviously a rank-two matrix, and the eigen-vectors corresponding to two non-zero eigen-values must be linear combinations of $\mathbf{g}(f_0,\boldsymbol{\theta}_{s0})$ and $\mathbf{g}(f_0,\boldsymbol{\theta}_{s1})$. That means,

$$\begin{aligned}&\left[\tfrac{1}{\alpha(f_0,\boldsymbol{\theta}_{s1})}\mathbf{g}(f_0,\boldsymbol{\theta}_{s1})\mathbf{g}^H(f_0,\boldsymbol{\theta}_{s1})-\tfrac{1}{\alpha(f_0,\boldsymbol{\theta}_{s0})}\mathbf{g}(f_0,\boldsymbol{\theta}_{s0})\mathbf{g}^H(f_0,\boldsymbol{\theta}_{s0})\right]\\&\mathbf{K}_{\mathbf{n}}^{-1}(f_0)\mathbf{K}_{\mathbf{r}}(f_0,\boldsymbol{\theta}_{s0})\mathbf{K}_{\mathbf{n}}^{-1}(f_0)\left(\mathbf{g}(f_0,\boldsymbol{\theta}_{s0})+\beta\mathbf{g}(f_0,\boldsymbol{\theta}_{s1})\right)\\&=\lambda\left(\mathbf{g}(f_0,\boldsymbol{\theta}_{s0})+\beta\mathbf{g}(f_0,\boldsymbol{\theta}_{s1})\right)\end{aligned}. \tag{28}$$

After some tedious but straightforward algebra, we have

$$\begin{aligned}&\mathbf{g}(f_0,\boldsymbol{\theta}_{s0})\cdot\\&\begin{bmatrix}\sigma_b^2(f_0)\mathbf{g}^H(f_0,\boldsymbol{\theta}_{s0})\mathbf{K}_{\mathbf{n}}^{-1}(f_0)\mathbf{g}(f_0,\boldsymbol{\theta}_{s0})+\\\beta\sigma_b^2(f_0)\mathbf{g}^H(f_0,\boldsymbol{\theta}_{s0})\mathbf{K}_{\mathbf{n}}^{-1}(f_0)\mathbf{g}(f_0,\boldsymbol{\theta}_{s1})+\lambda\end{bmatrix}\\&-\\&\mathbf{g}(f_0,\boldsymbol{\theta}_{s1})\cdot\\&\begin{bmatrix}\sigma_b^2(f_0)\frac{\alpha(f_0,\boldsymbol{\theta}_{s0})}{\alpha(f_0,\boldsymbol{\theta}_{s1})}\mathbf{g}^H(f_0,\boldsymbol{\theta}_{s1})\mathbf{K}_{\mathbf{n}}^{-1}(f_0)\mathbf{g}(f_0,\boldsymbol{\theta}_{s0})+\\\beta\begin{pmatrix}\frac{\sigma_b^2(f_0)}{\alpha(f_0,\boldsymbol{\theta}_{s1})}\mathbf{g}^H(f_0,\boldsymbol{\theta}_{s1})\mathbf{K}_{\mathbf{n}}^{-1}(f_0)\mathbf{g}(f_0,\boldsymbol{\theta}_{s0})\cdot\\\mathbf{g}^H(f_0,\boldsymbol{\theta}_{s0})\mathbf{K}_{\mathbf{n}}^{-1}(f_0)\mathbf{g}(f_0,\boldsymbol{\theta}_{s1})\\+\frac{1}{\alpha(f_0,\boldsymbol{\theta}_{s1})}\mathbf{g}^H(f_0,\boldsymbol{\theta}_{s1})\mathbf{K}_{\mathbf{n}}^{-1}(f_0)\mathbf{g}(f_0,\boldsymbol{\theta}_{s1})-\lambda\end{pmatrix}\end{bmatrix}\\&=0\end{aligned}. \tag{29}$$

The coefficients of $\mathbf{g}(f_0,\boldsymbol{\theta}_{s0})$ and $\mathbf{g}(f_0,\boldsymbol{\theta}_{s1})$ must both be zero. Solving β from the coefficient of $\mathbf{g}(f_0,\boldsymbol{\theta}_{s0})$ and substituting it to the coefficient of $\mathbf{g}(f_0,\boldsymbol{\theta}_{s1})$ yield a quadratic equation of λ:

$$\begin{aligned}&(1+\Sigma_{11})\lambda^2+\left(\Sigma_{00}-\Sigma_{11}+\Sigma_{00}\Sigma_{11}-\left|\Sigma_{01}\right|^2\right)\lambda\\&+\left(\left|\Sigma_{01}\right|^2-\Sigma_{00}\Sigma_{11}\right)=0\end{aligned}, \tag{30}$$

where

$$\Sigma_{00}=\sigma_b^2(f_0)\mathbf{g}^H(f_0,\boldsymbol{\theta}_{s0})\mathbf{K}_{\mathbf{n}}^{-1}(f_0)\mathbf{g}(f_0,\boldsymbol{\theta}_{s0}), \tag{31}$$

$$\Sigma_{11}=\sigma_b^2(f_0)\mathbf{g}^H(f_0,\boldsymbol{\theta}_{s1})\mathbf{K}_{\mathbf{n}}^{-1}(f_0)\mathbf{g}(f_0,\boldsymbol{\theta}_{s1}), \tag{32}$$

$$\Sigma_{01}=\sigma_b^2(f_0)\mathbf{g}^H(f_0,\boldsymbol{\theta}_{s1})\mathbf{K}_{\mathbf{n}}^{-1}(f_0)\mathbf{g}(f_0,\boldsymbol{\theta}_{s0}). \tag{33}$$

The eigen-values are then solved in a standard form:

$$\begin{aligned}&\lambda_{1,2}(f_0,\boldsymbol{\theta}_{s0},\boldsymbol{\theta}_{s1})=\\&\frac{-1}{2(1+\Sigma_{11})}\begin{pmatrix}\left(\Sigma_{00}-\Sigma_{11}+\Sigma_{00}\Sigma_{11}-\left|\Sigma_{01}\right|^2\right)\\\pm\sqrt{\left(\Sigma_{00}+\Sigma_{11}+\Sigma_{00}\Sigma_{11}-\left|\Sigma_{01}\right|^2\right)^2-4\left|\Sigma_{01}\right|^2}\end{pmatrix}\end{aligned}. \tag{34}$$

Note that $\lambda_1<0$ and $\lambda_2>0$. The statistics is now stated by

$$\gamma(f_0,\boldsymbol{\theta}_{s0},\boldsymbol{\theta}_{s1})=\mathrm{tr}\left(\mathbf{Z}(f_0)\mathbf{Z}^H(f_0)\mathbf{U}^H\boldsymbol{\Lambda}\mathbf{U}\right). \tag{35}$$

Since $\mathbf{U}$ is a unitary matrix, $\mathbf{UZ}$ shares the same distribution with $\mathbf{Z}$ [4] and thus

$$\begin{aligned}&\gamma(f_0,\boldsymbol{\theta}_{s0},\boldsymbol{\theta}_{s1})\\&\overset{d}{=}\mathrm{tr}\left(\mathbf{Z}(f_0)\mathbf{Z}^H(f_0)\boldsymbol{\Lambda}(f_0)\right),\\&\overset{d}{=}\lambda_1\cdot\chi_{1,L}^2+\lambda_2\cdot\chi_{2,L}^2\end{aligned} \tag{36}$$

which is a weighted sum of two independent degree-L complex Chi-squared variables.

Now the error probability is

$$\mathrm{P_e}(\boldsymbol{\theta}_{s1}|\boldsymbol{\theta}_{s0})=\Pr\left(l'=\lambda_1\cdot\chi_{1,L}^2+\lambda_2\cdot\chi_{2,L}^2\geq L\ln\tfrac{\alpha(f_0,\boldsymbol{\theta}_{s0})}{\alpha(f_0,\boldsymbol{\theta}_{s1})}\right). \tag{37}$$

The pdf of l' is derived in Ref. [4], which is

$$p(l')=\begin{cases}\sum_{k=1}^{L}\frac{C_{k+}}{(k-1)!}(-1)^k l'^{k-1}e^{-l'/\lambda_2} & l'>0\\\sum_{k=1}^{L}\frac{C_{k-}}{(k-1)!}(-l')^{k-1}e^{-l'/\lambda_1} & l'<0\end{cases}, \tag{38}$$

where C_{k+} and C_{k-} are partial expansion coefficients of the moment generating function of l', i.e.,

$$\Phi_{l'}(s)=\left(\frac{\frac{1}{\lambda_1}}{s-\frac{1}{\lambda_1}}\right)^L\left(\frac{\frac{1}{\lambda_2}}{s-\frac{1}{\lambda_2}}\right)^L, \tag{39}$$

$$C_{k+}=\frac{1}{(L-k)!}\left[\frac{\partial^{L-k}}{\partial s^{L-k}}\left(\left(s-\frac{1}{\lambda_2}\right)^L\Phi_{l'}(s)\right)\right]_{s=1/\lambda_2}, \tag{40}$$

$$C_{k-}=\frac{1}{(L-k)!}\left[\frac{\partial^{L-k}}{\partial s^{L-k}}\left(\left(s-\frac{1}{\lambda_1}\right)^L\Phi_{l'}(s)\right)\right]_{s=1/\lambda_1}. \tag{41}$$

Define $\eta=L\ln\frac{\alpha(f_0,\boldsymbol{\theta}_{s0})}{\alpha(f_0,\boldsymbol{\theta}_{s1})}$. The error probability is then

$$\begin{aligned}\mathrm{P_e}(\boldsymbol{\theta}_{s1}|\boldsymbol{\theta}_{s0})&=\Pr\left(l'\geq\eta\right)=\int_\eta^\infty p(l')dl'\\&=\int_0^\infty p(l')dl'-\int_0^\eta p(l')dl'\end{aligned}. \tag{42}$$

Solving the integration, we finally have

$$
\mathrm{P_e}(\boldsymbol{\theta}_{s1}|\boldsymbol{\theta}_{s0}) = \begin{cases} e^{-\eta}\sum_{k=1}^{L}\left(C_{k+}(-\lambda_2)^k\sum_{j=0}^{k-1}\frac{\eta^j}{j!}\right) \\ \qquad\qquad\qquad\qquad \eta > 0 \\ \sum_{k=1}^{L}\left(C_{k+}(-\lambda_2)^k + C_{k-}(-\lambda_1)^k\left(1-e^{-\eta}\sum_{j=0}^{k-1}\frac{\eta^j}{j!}\right)\right) \\ \qquad\qquad\qquad\qquad \eta < 0 \end{cases} . \quad (43)
$$

The error probability in (43) is solely determined from (31), (32) and (33). The first two define the signal self-correlation referenced in the space of additive noise, i.e., signal-to-noise ratio at both source locations; the last one defines a cross-correlation term referenced in the same space, i.e., signal ambiguity level projected onto the noise space. The exact way those terms act on the error probability is not clear and to be studied. However, we would expect that for a fixed SNR level the error probability is high when the projected correlation associated with two chosen parameter points is high; for a fixed pair of parameter points (and thus fixed projected correlation), the error probability increases as the SNR decreases.

When we set the correlated noise term to zero, Eq. (43) yields the error probability for white noise process, which is investigated in Ref. [1]. The result here, however, is more accurate because no assumption is made on the parameter-independence of the norm of the signal replica.

V. Summary and Discussions

In this paper, we generalize the previously-developed matched-field ambiguity analysis to include spatially-correlated noise field. This is done by deriving the error probability of the likelihood ratio test under spatially-correlated noise field. The new development represents a further effort to apply quantitative error analysis to matched-field methods in more realistic environments.

Given the data model in (1), the signal-to-noise ratio can be defined as

$$
\mathrm{SNR}(f) = \frac{\mathrm{tr}\left(\sigma_b^2(f)\mathbf{g}(f,\boldsymbol{\theta}_s)\mathbf{g}^H(f,\boldsymbol{\theta}_s)\right)}{\mathrm{tr}\left(\mathbf{K_n}(f)\right)} . \quad (44)
$$

One might want to look at the mean-square error as a function of the white noise variance with fixed correlated noise contribution; one can also look at the mean-square error as a function of correlated noise term, like that described by the Kuperman-Ingenito (KI) surface noise model [10], with fixed white noise contribution. Another interesting application is to look at performance when correlated noise is from a surface ship interferer and find out how the performance degrades as signal of interest approach ship. Some of these issues are currently being investigated.

We should also point out that there is an underlying assumption that the CRB describes the asymptotic MSE performance. This is not always the case in colored noise. For example, a mainlobe discrete interferer can cause main peak of ambiguity function to be at place other than true parameter value, introducing a bias asymptotically. The CRB can be modified to account for this bias [9, pages 146-147].

References

[1] W. Xu, A. B. Baggeroer, and H. Schmidt, "Quantitative ambiguity analysis for matched-field source localization," *Proc. 36th Asilomar Conference on Signals, Systems, and Computers*, pp448-452, 2002.

[2] A. B. Baggeroer, W. A. Kuperman, and P. N. Mikhalevsky, "An overview of matched field methods in ocean acoustics," *IEEE J. Oceanic Engineering*, Vol. 18, pp401-424, 1993.

[3] J. Tabrikian and J. L. Krolik, "Barankin bounds for source localization in an uncertain ocean environment," *IEEE Trans. Signal Processing*, Vol. 47, pp2917-2927, 1999.

[4] W. Xu, "Performance Bounds on Matched-Field Methods for Source Localization and Estimation of Ocean Environmental Parameters", Ph.D. dissertation, Massachusetts Institute of Technology, Cambridge, MA, 2001.

[5] F. Athley, "Performance analysis of DOA estimation in the threshold region," *Proc. ICASSP*, 2002.

[6] F. Athley, "Threshold region performance of deterministic maximum likelihood DOA estimation of multiple sources," *Proc. 36th Asilomar Conference on Signals, Systems, and Computers*, 2002.

[7] C. D. Richmond, "Mean square error performance prediction of maximum-likelihood signal parameter estimation," *Proc. 11th Adaptive Sensor Array Processing Workshop*, MIT Lincoln Lab, 2003.

[8] A. B. Baggeroer and H. Schmidt, "Cramer-Rao bounds for matched field tomography and ocean acoustic tomography," *Proc. ICASSP*, pp2763-2766, 1995.

[9] H. L. Van Trees, *Detection, Estimation, and Modulation Theory, Part I*, New York: John Wiley & Sons, 1968.

[10] W. A. Kuperman and F. Ingenito, "Spatial correlation of surface generated noise in a stratified ocean," J. Acoust. Soc. Am., Vol. 67, pp1988-1996, 1980.